



Additional Evidence for Low Mass Exotic Baryons

B. Tatischeff, E. Tomasi-Gustafsson

► To cite this version:

B. Tatischeff, E. Tomasi-Gustafsson. Additional Evidence for Low Mass Exotic Baryons. 11th International Conference on Nuclear Reaction Mechanisms, Jun 2006, Varenna, Italy. pp.339-348. in2p3-00125255

HAL Id: in2p3-00125255

<https://hal.in2p3.fr/in2p3-00125255>

Submitted on 18 Jan 2007

HAL is a multi-disciplinary open access archive for the deposit and dissemination of scientific research documents, whether they are published or not. The documents may come from teaching and research institutions in France or abroad, or from public or private research centers.

L'archive ouverte pluridisciplinaire **HAL**, est destinée au dépôt et à la diffusion de documents scientifiques de niveau recherche, publiés ou non, émanant des établissements d'enseignement et de recherche français ou étrangers, des laboratoires publics ou privés.

Additional Evidence for Low Mass Exotic Baryons

B. Tatischeff^{1*}

Institut de Physique Nucléaire
CNRS/IN2P3, F-91406 Orsay Cedex, France

E. Tomasi-Gustafsson^{2†}

DAPNIA/SPhN, CEA/Saclay
91191 Gif-sur-Yvette Cedex, France

This paper aims to give further evidence for the existence of low mass exotic baryons. It consists of two parts:

- first it recalls some results, already shown or even previously published, which reflect the existence of narrow low mass baryonic states,
- then it presents new results obtained through the analysis of recent data from JLAB. We will show that these results are compatible with our previous observation, namely that the broad PDG baryonic resonances can be shared into several more narrow ones .

1 Already shown (*although not always known*) results

The first observation of narrow baryonic structures was done nine years ago in the missing mass of the $pp \rightarrow p\pi^+X$ reaction at Saturne (SPES3 beam line) [1]. Fig. 1 shows the presence of small narrow structures, located between the neutron and the $\Delta(3,3)$ missing mass peaks. These structures were observed at nearly all angles and incident energies available. Later on, smaller structures were observed at other masses, in the missing mass and invariant mass of the previous reaction as well as in $pp \rightarrow ppX$ reaction. The results concerning the $1.0 \leq M \leq 1.46$ GeV mass range [2], then the $1.47 \leq M \leq 1.68$ GeV mass range [3], pointed out to the presence of several narrow and weakly excited structures. These structures were observed at the same masses, indicating that we observe genuine baryonic states.

In the mass range $1.47 \leq M \leq 1.68$ GeV, we suggest, see fig. 2, that the broad PDG baryonic resonances are collective states of several weakly excited and narrow resonances, which can be single-particle-or-quasi-particle states, more complicated than $|q >^3$. The reason for which the PDG resonances have so large widths may be due to the lack of experimental precision in previous experiments.

We observe sometimes, in previously published data by various authors, narrow discontinuities in their spectra, which were not discussed. This is observed as well for reactions using incident hadron beams, as for reactions using lepton beams. However the structures below pion production threshold are not observed in reactions using incident leptons. The authors of these papers, where data exhibit small and narrow structures, did not take into account the possibility to associate the discontinuities of their spectra with possible narrow baryonic low mass structures. Fig. 3 shows one of the most striking example: the $p(\alpha, \alpha')X$ reaction was studied at SPES4 (Saturne) in order to study the excitation of the Roper resonance. Above projectile and target excitations, both histograms taken at $\theta=0.8^\circ$ [4]

*e-mail : tati@ipno.in2p3.fr

†e-mail : etomasi@cea.fr

and 2^0 [5], exhibit well statistically defined structures. Their masses agree with the masses observed in the SPES3 data [3] (see fig. 4).

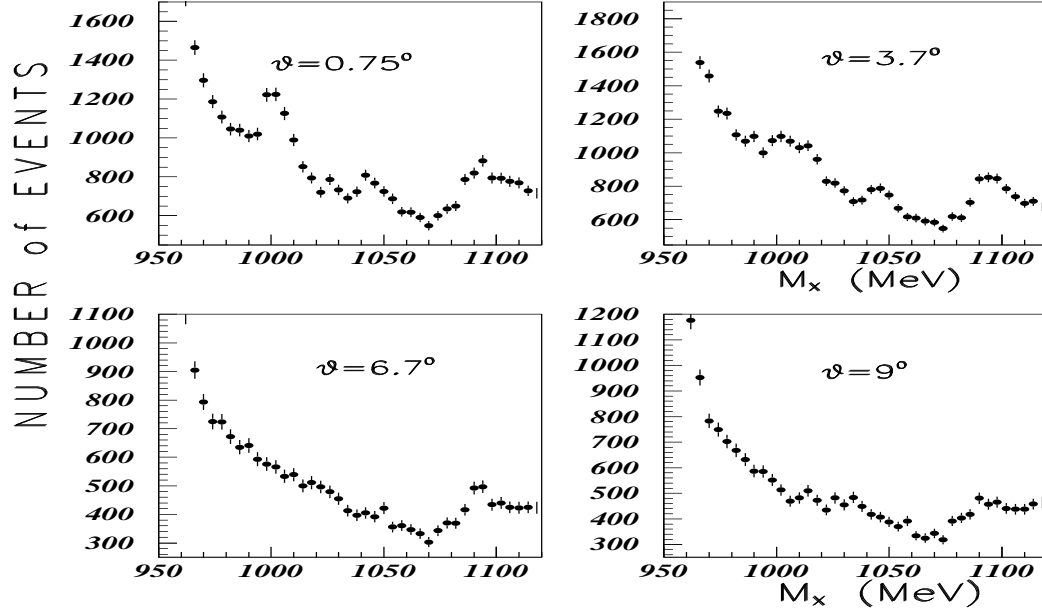


Figure 1: Missing mass spectra of the $pp \rightarrow p\pi^+X$ reaction [1] measured at SPES3 (Saturne).

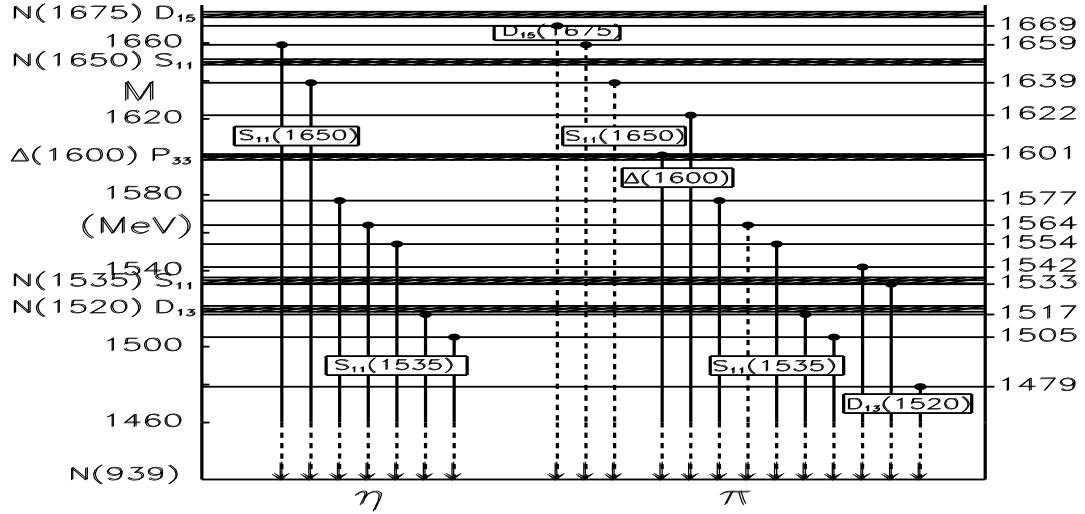


Figure 2: Disintegration channels of the narrow baryonic resonances experimentally observed [3] and attempt to associate them with broad PDG resonances using the disintegration channels $p\eta$ and $p\pi$, or $p\pi$ alone.

Fig. 5 illustrates some narrow structures observed with leptons. Inserts (a) and (b) show low energy Compton scattering from the proton, measured at Saskatchewan [6]. A narrow structure is observed, close to $M=1094$ MeV. A structure at the same mass was extracted from SPES3 data. Insert (c) shows a narrow peak at $M=1050$ MeV in the Compton scattering data measured at Mainz [7]. This mass is close to $M=1044$ MeV (SPES3 value). The Mainz cross-sections at $\theta=59^\circ$, 85° , 107° , 135° , and 155° are added, in order to reduce the statistical errors. Insert (d) shows a small peak corresponding to a narrow dibaryon at $M=2053.4$ MeV observed in data from JLAB [8]. This value is very close to the SPES3 mass $M=2052$ MeV.

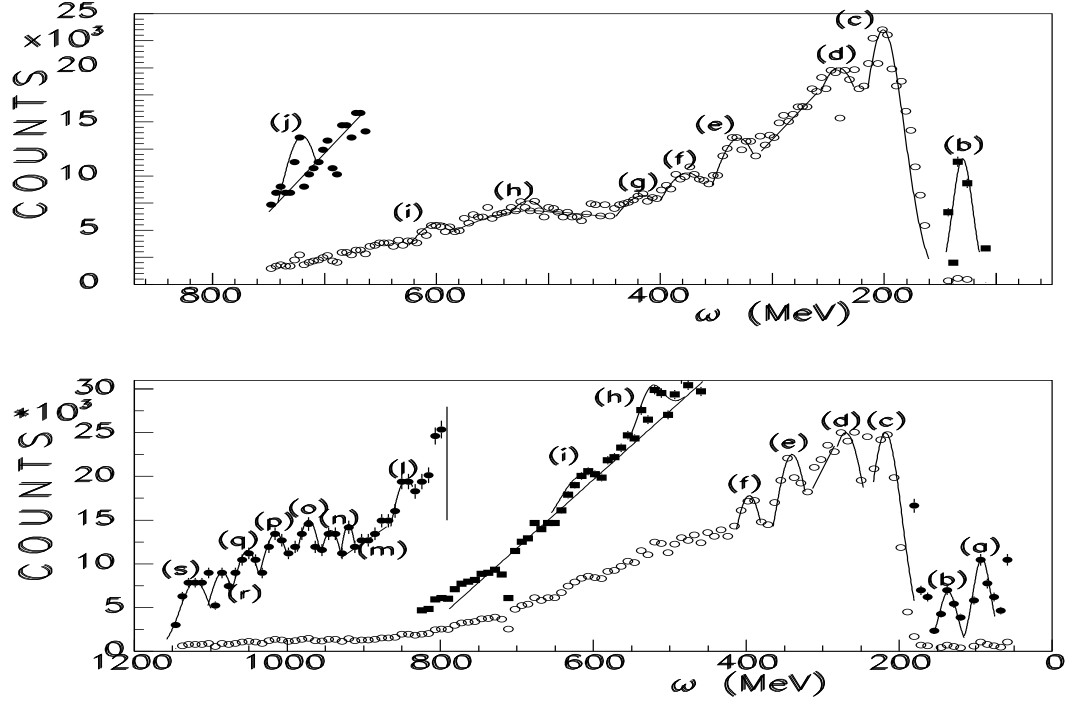


Figure 3: $p(\alpha, \alpha')X$ spectra at $T_\alpha=4.2$ GeV, $\theta = 0.8^\circ$ in upper insert [4], and $\theta = 2^\circ$ in lower insert [5], measured at SPES4 (Saturne).

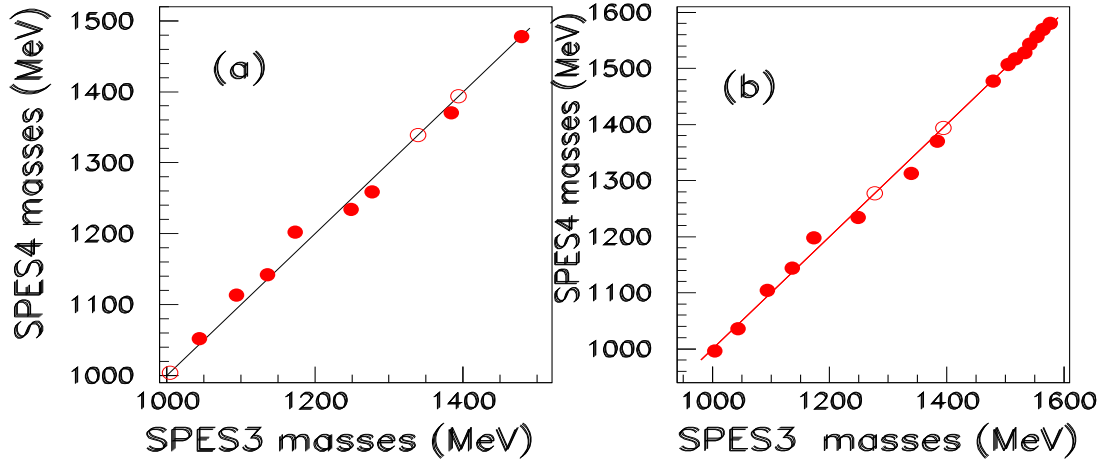


Figure 4: Comparison between masses of narrow baryons extracted from SPES3 and SPES4 data. Inserts (a) and (b) correspond respectively to $\theta=0.8^\circ$ [4] and $\theta=2^\circ$ [5].

2 Analysis of recent data from JLAB

Three reactions of virtual photons scattered on protons are discussed here:

- $ep \rightarrow e'p\gamma$ [9] studied by the Hall A Collaboration
- $ep \rightarrow e'p\pi^0$ [10] studied by the Hall A Collaboration.
- $ep \rightarrow e'n\pi^+$ [11] studied by the CLAS Collaboration,

The two last experiments have measured the same (except isospin) structure functions, but at different kinematical values of Q^2 , and θ^* . The corresponding data are presented with 20 MeV bins. The resolution is better in Hall A than in CLAS, but in both cases it is not well suited for the study of narrow structures since the experiments were not performed

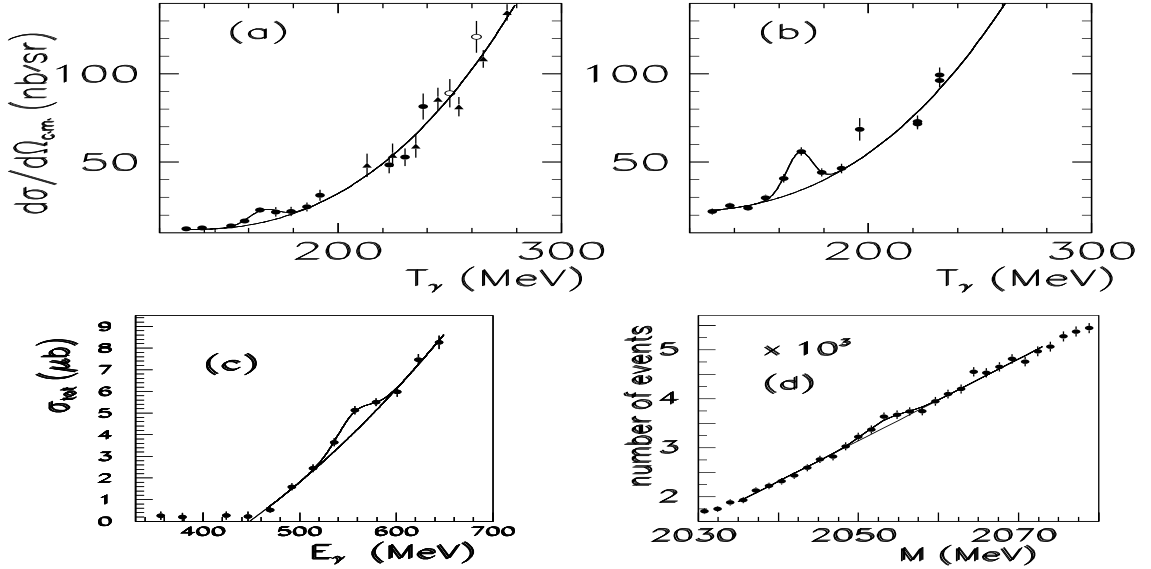


Figure 5: Narrow hadrons produced by leptons. Inserts (a) ($\theta = 90^\circ$) and (b) ($\theta = 141^\circ$) show cross-sections of Compton scattering from the proton [6], insert (c) shows total cross-section of Compton scattering [7](see text). Insert (d) shows a narrow dibaryonic peak observed at $\theta_e \approx 20^\circ$ in the ed scattering data [8], with $E_e = 4.05$ GeV (see text).

for such study. These structures can be found in spectra corresponding to many different kinematical conditions; a selection among the many histograms is done for the present discussion.

Some figures presented later exhibit structures below and above $M=1230$ MeV. Since there is no PDG broad resonance with the same quantum numbers as those of N , before $M=1440$ MeV, such results cannot be attributed to interferences between several PDG resonances. An interference between the $\Delta(1230)P_{33}$ and the non resonant background is possible, but it will unlikely give rise to several narrow oscillations as those observed in several figures shown later. It is likely that the non-resonant background amplitudes vary slowly and steadily for increasing baryonic masses. Alternative explanation, consistent with previous observations [3], is the existence of some narrow baryonic states in the mass region discussed here. We have not adjusted the masses and have kept those found in the analysis of the SPES3 data (two structures at $M=1173$ MeV and $M=1249$ MeV are described here by one structure at $M=1220$ MeV). A constant gaussian width is kept for each set of data. In the discussion concerning the $\gamma^*p \rightarrow p\pi$ reactions, we compare the experimental data to the calculations performed with the MAID model [12].

2.1 $ep \rightarrow e'p\gamma$

The virtual Compton scattering cross sections were measured by the Hall A Collaboration [9]. They are given at backward angles versus the mass of the hadronic system (C.M.S.). No background was subtracted. It was shown [9] that the BH+Born as well as BH+Born+ π^0 exchange cross sections are smooth. Fig. 6 shows, for three different kinematical conditions, the need of several narrow structures to describe the histograms. The masses are those extracted from the SPES3 results. The same width (FWHM=36 MeV) allows to get a good fit, when only the heights of the peaks are varied. More results of the same quality are available in several different kinematical conditions and always the structures are extracted at the same positions.

The mass values are: α :1004 MeV, β :1044 MeV, γ :1094 MeV, δ :1136 MeV, ϵ :1173 MeV, η :1212 MeV, ϕ :1249 MeV, λ :1277 MeV, and μ :1339 MeV. We observe in (a) a well defined

(β) structure, and the absence of a $\Delta(1220)$ peak. All three inserts display an oscillatory behaviour, specially for the first lower mass structures. A $\Delta(1220)$ peak exists in insert (c) but with a width much lower than $\Gamma_{1/2}=120$ MeV. Such approach ignores all interferences, otherwise the number of free parameters will strongly increase.

In order to enhance the precision, the cross sections at different Φ values are added. Φ is the azimuthal angle between the leptonic and the hadronic planes. Fig. 7 shows, that the same comments as those done for Fig. 6, can be done for data plotted in insert (b): narrow β peak and nearly no $\Delta(1220)$ peak. Six different cross sections corresponding to different Φ angles are added in fig. 8 for $Q^2 = 1 \text{ GeV}^2$ and $\cos(\theta_{\gamma\gamma}^*)=-0.975$. The Δ peak, if considered alone, is located here at $M=1194$ MeV, a value too low by $\Delta M \approx 30$ MeV (FWHM=118 MeV). It is plotted with a dashed line, as well as the nucleon peak. It is unlikely to have, in the context of the PDG baryons, any coherent contribution between 1.0 and 1.2 GeV since there is no interference between N and Δ . An interference with non coherent background is possible but we observe that the experimental cross section is larger than half the Δ cross section.

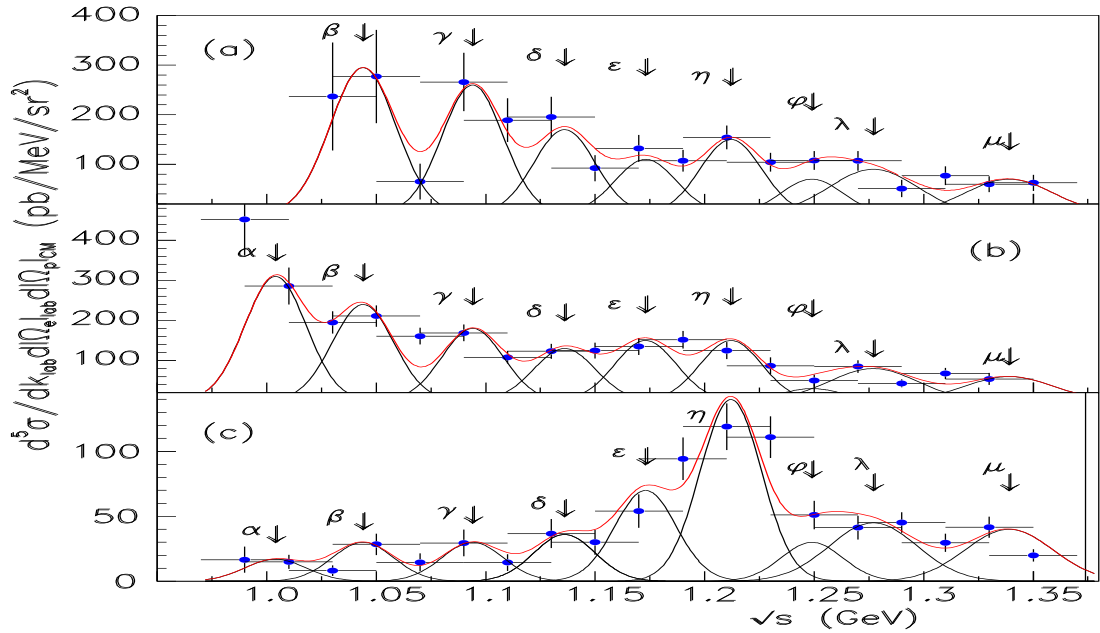


Figure 6: Cross sections of the $\gamma^*p \rightarrow \gamma p$ reaction [9] at $Q^2 = 1 \text{ GeV}^2$. Inserts (a), (b), and (c) correspond respectively to the following kinematical conditions: $\cos(\theta_{\gamma\gamma}^*)=-0.65$, $\Phi = 45^\circ$, $\cos(\theta_{\gamma\gamma}^*)=-0.65$, $\Phi = 105^\circ$, and $\cos(\theta_{\gamma\gamma}^*)=-0.975$, $\Phi = 15^\circ$.

The extracted yields of the narrow structures are continuous and are well fitted by the formula $d^2\sigma/d\Omega_\pi^* = a + b \cos(\Phi) + c \cos(2\Phi)$. Fig. 9 shows these fits.

2.2 $ep \rightarrow e'p\pi^0$

Backward π^0 electroproduction on protons were measured by the Hall A Collaboration [10]. No background is introduced in the figures corresponding to this subsection, since the cross sections of the interference structure functions versus W , the mass of the hadronic system, present positive as well as negative values. Fig. 10 shows, in the four inserts, the cross section of the same structure function σ_{TT} at $Q^2=1 \text{ GeV}^2$ at four backward polar angles: $\cos(\theta^*)=-0.975$ (a), -0.925 (b), -0.875 (c), and -0.825 (d).

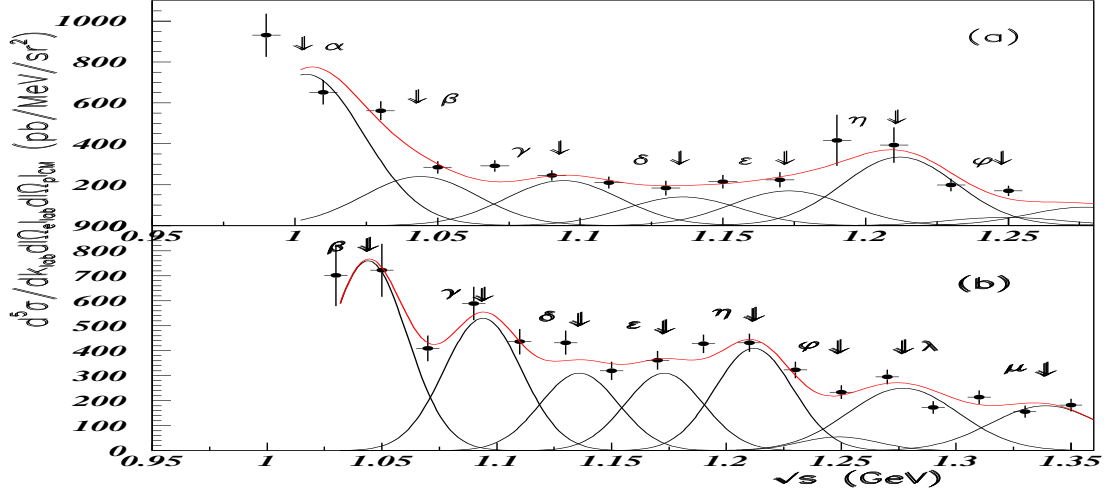


Figure 7: Cross sections of the $\gamma^*p \rightarrow \gamma p$ reaction [9] at $Q^2 = 1 \text{ GeV}^2$. Both inserts correspond respectively to the following kinematical conditions. (a): $\cos(\theta_{\gamma\gamma}) = -0.875$ and $\Phi = 135^\circ$ plus $\Phi = 165^\circ$, (b): $\cos(\theta_{\gamma\gamma}^*) = -0.65$ and $\Phi = 45^\circ$ plus $\Phi = 75^\circ$ plus $\Phi = 105^\circ$.

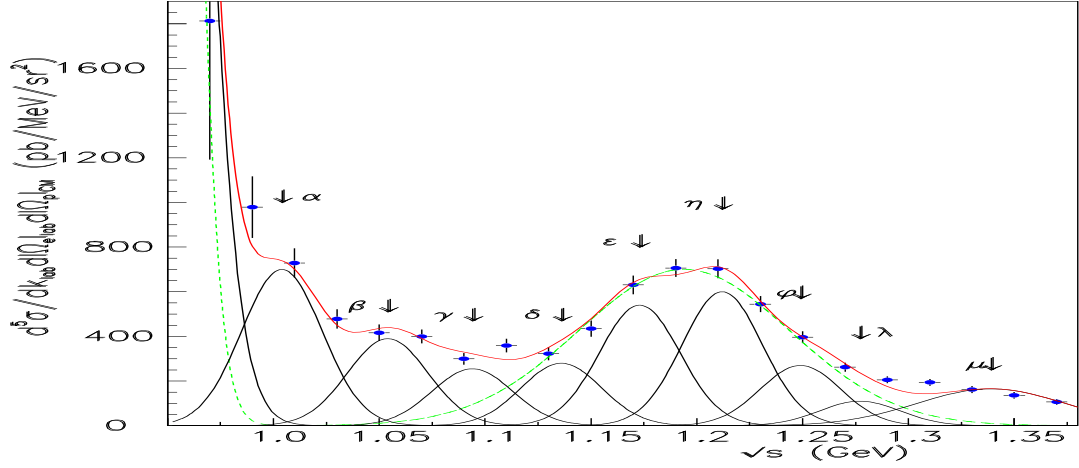


Figure 8: Cross sections of the $\gamma^*p \rightarrow \gamma p$ reaction [9] at $Q^2 = 1 \text{ GeV}^2$ and $\cos(\theta_{\gamma\gamma}^*) = -0.975$ (see text).

A good adjustment is obtained with again the same narrow structure masses as before, and a common width $\text{FWHM} = 56 \text{ MeV}$. Here the oscillatory structure is not present, but the width of a single gaussian, would be close to $\text{FWHM} = 66 \text{ MeV}$ (dashed line), and not 120 MeV as quoted in PDG.

Fig. 11 shows the $d\sigma_T/d\Omega + \epsilon d\sigma_L/d\Omega$ structure function for the same kinematical conditions as in fig. 10. In these two figures the dashed lines show the MAID results. Although the global shape is reproduced, we observe a decrease of the quantitative agreement with decreasing angles and, of course, the missing of the small experimental structures in the $1.35 \leq M \leq 1.43 \text{ GeV}$ range.

2.3 $ep \rightarrow e'n\pi^+$

Some cross sections of the structure functions from $ep \rightarrow e'n\pi^+$ reaction, measured by the CLAS Collaboration [11], are plotted versus the mass of the hadronic system W . No background is subtracted, here again, since the cross sections of the interference structure functions present positive and negative values. Fig. 12 shows three cross-section corresponding to the following structure functions:

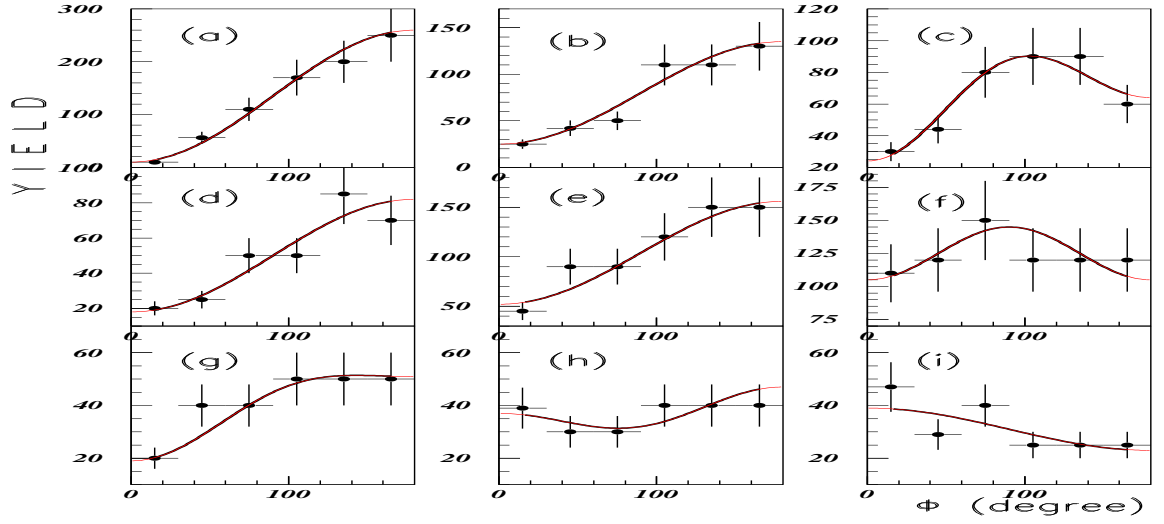


Figure 9: Fits versus Φ of the narrow structures (a): 1004 MeV, (b): 1044 MeV, (c): 1094 MeV, (d): 1136 MeV, (e): 1173 MeV, (f): 1212 MeV, (g): 1249 MeV, (h): 1277 MeV, and (i): 1339 MeV (see text).

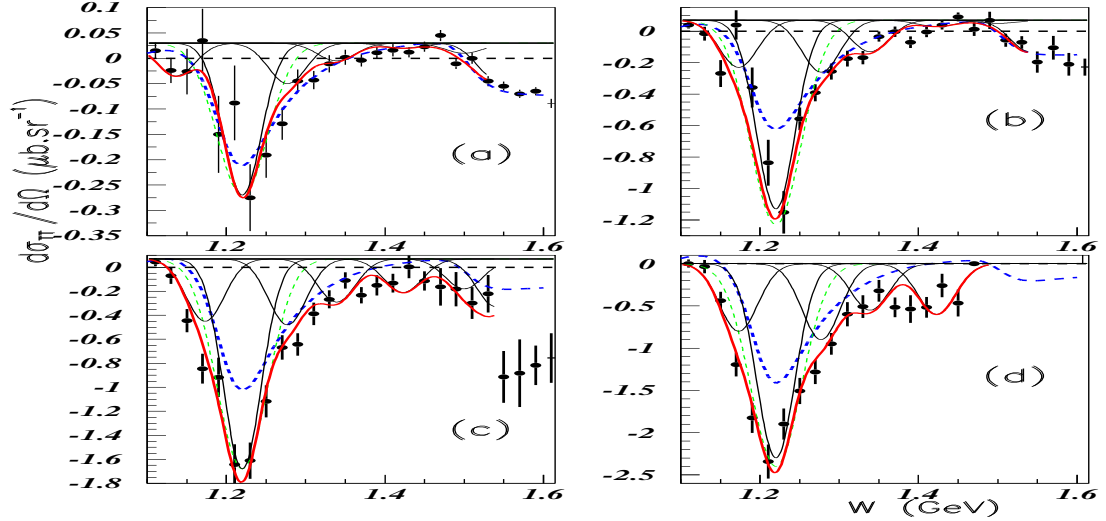


Figure 10: Cross sections of the σ_{TT} structure function [10] corresponding to the backward π^0 electroproduction on p at $Q^2 = 1 \text{ GeV}^2$ (see text).

$\sigma_T + \epsilon \sigma_L$, σ_{TL} , and σ_{TT} corresponding to four transfer squared $Q^2=0.4 \text{ GeV}^2$ and $\theta_{\gamma\gamma} = 22.5^\circ$. The FWHM of the main peak, for inserts (a), (b), and (c), equal respectively 235 MeV, 57 MeV, and 61 MeV, when the analysis with the same structure masses as before, and again a single width (FWHM=82 MeV), allows good fits.

Fig. 13 shows the $\sigma_T + \epsilon \sigma_L$ structure function at $\theta=7.5^\circ$ and $Q^2=0.3 \text{ GeV}^2$ in insert (a) and $Q^2=0.4 \text{ GeV}^2$ in insert (b); and the σ_{TT} structure functions at $\theta=37.5^\circ$ and $Q^2=0.3 \text{ GeV}^2$ in insert (c) and $Q^2=0.4 \text{ GeV}^2$ in insert (d). The dashed curves correspond to MAID. We observe that the MAID results miss a large part of the experimental spectra, mainly in fig. 12(b), 12(c), 13(a), 13(c), and 13(d).

Fig.14 shows at $Q^2=0.3 \text{ GeV}^2$, the σ_{TL} in insert (a) and σ_{TT} insert(b) at $\theta=52.5^\circ$, and the same for $\theta=67.5^\circ$ in inserts (c) and (d). The data are not correctly reproduced by MAID for $W \geq 1280 \text{ MeV}$ in inserts (a) and (b).

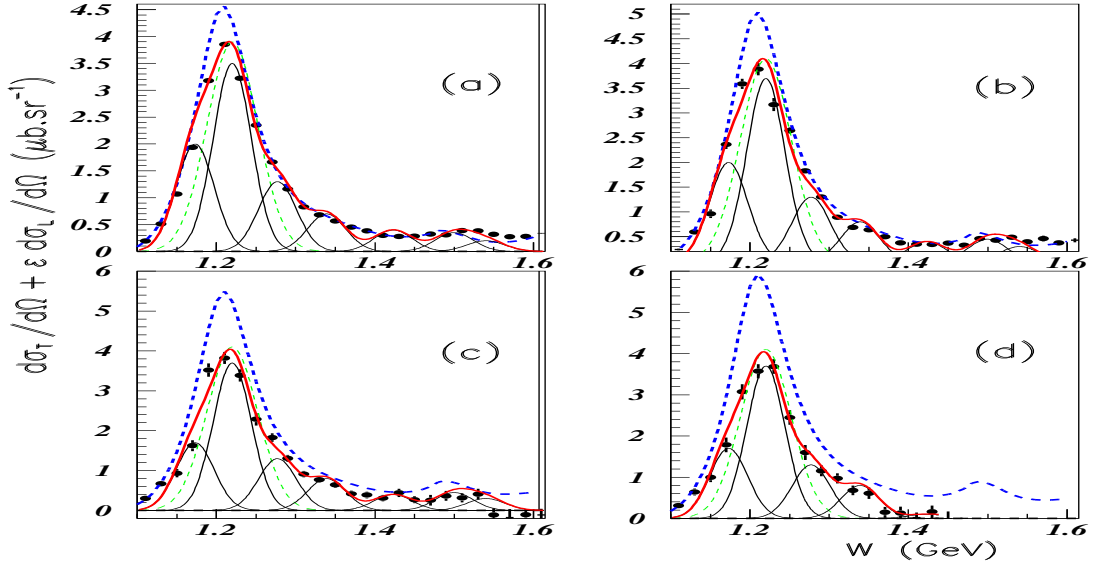


Figure 11: Cross sections of the σ_{TT} structure function [10] corresponding to the backward π^0 electroproduction on p at $Q^2 = 1 \text{ GeV}^2$ (see text).

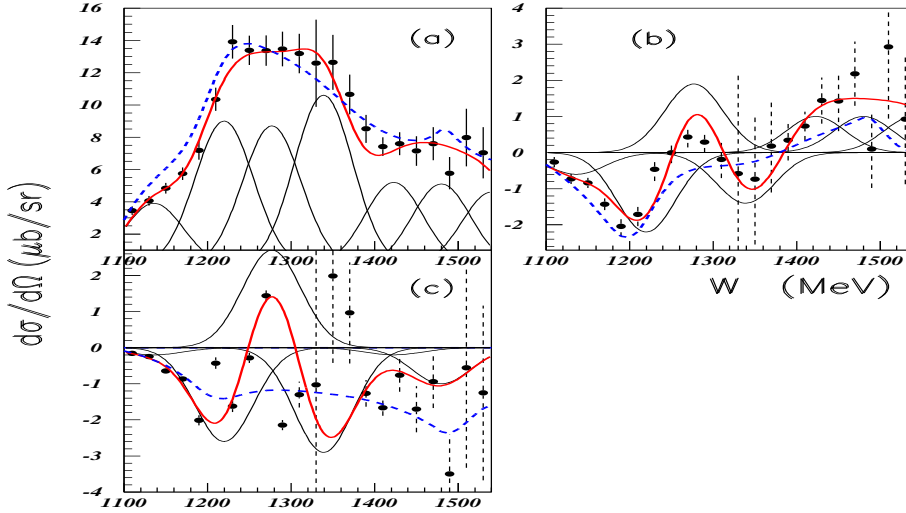


Figure 12: Cross section of the structure functions from the $ep \rightarrow e'n\pi^+$ reaction [11] measured at $Q^2=0.4 \text{ GeV}^2$, $\theta=22.5^\circ$ (see text).

It is necessary, in order to strengthen these decompositions, to verify the continuity of the narrow peak surfaces, for different angles θ . This is tentatively done in fig. 15: the left (right) part of the figure, shows the σ_{TT} (σ_{TL}) results. We observe the close values obtained from the $Q^2=0.4 \text{ GeV}^2$ (full circles) and $Q^2=0.3 \text{ GeV}^2$ (empty circles) structure functions. We observe also a good continuity for increasing angles. The curves are fitted according to $d\sigma/d\Omega = \sum_n A_n \cos^n \theta$. An arbitrary error of 20% was applied on all points. The dashed curves show the angular distribution corresponding to $l=1$, $J=3/2$ quantum numbers. We see that such contribution fit correctly the data for the structure at $M=1220 \text{ MeV}$ (and above $M=1400 \text{ MeV}$) in σ_{TT} cross section, and fit only the $M=1136 \text{ MeV}$ structure in the σ_{TL} cross section. Insert (a) of the σ_{TT} structure function, is well fitted with a distribution of the form: $1-\cos(\theta)$, like the inserts (b) and (d) of σ_{TL} . We tentatively conclude that these structures have different quantum numbers.

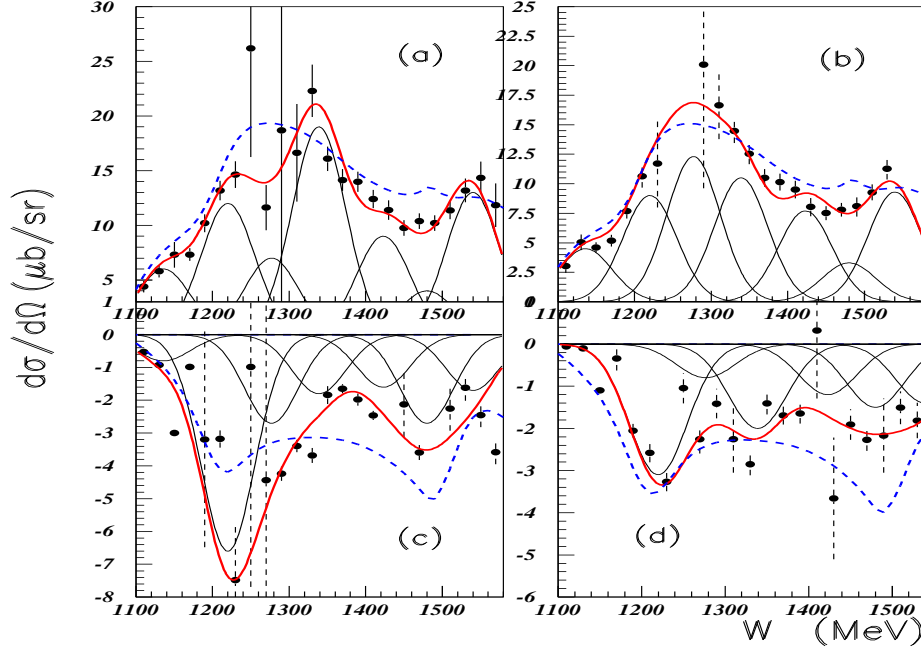


Figure 13: Cross section of the structure functions from the $ep \rightarrow e'n\pi^+$ reaction [11] (see text).

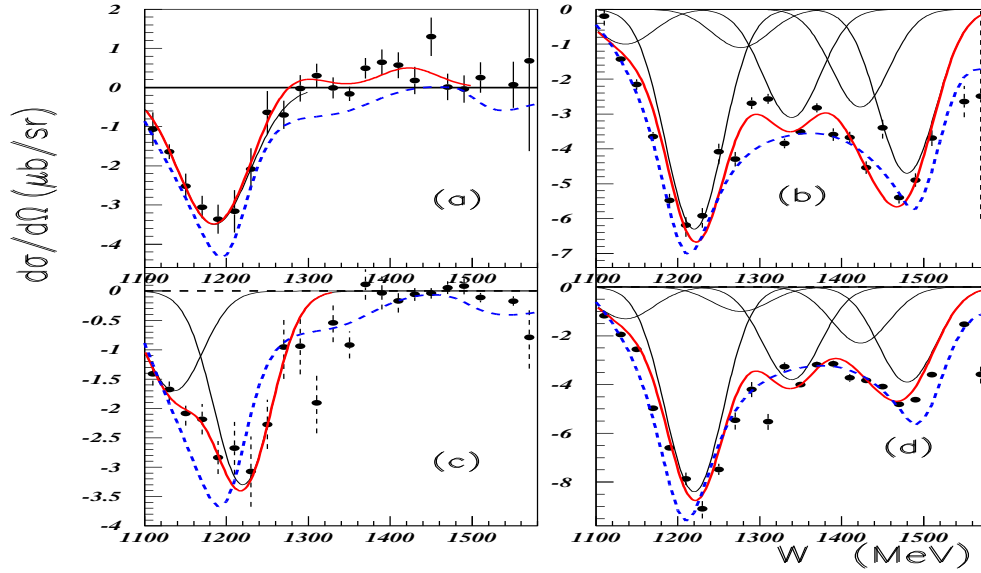


Figure 14: Cross section of the structure functions from the $ep \rightarrow e'n\pi^+$ reaction [11] (see text).

3 Conclusion

We have shown the existence of many narrow low mass baryonic states, which renew the importance of the study of baryon spectroscopy. Indeed, narrow structures are observed by different groups, in different reactions and different laboratories.

These states are exotic since there is no room for them, within the $|q >^3$ models. Some simple phenomenological mass formula were proposed which involve the existence of $q\bar{q}$ pairs (see references in [2]). A real theoretical study does not exist today. New dedicated experiments are needed, with large statistics, small bins and good resolution, typically $\Delta M \leq 5$ MeV.

We suggest that the broad PDG baryonic resonances are collective states of several

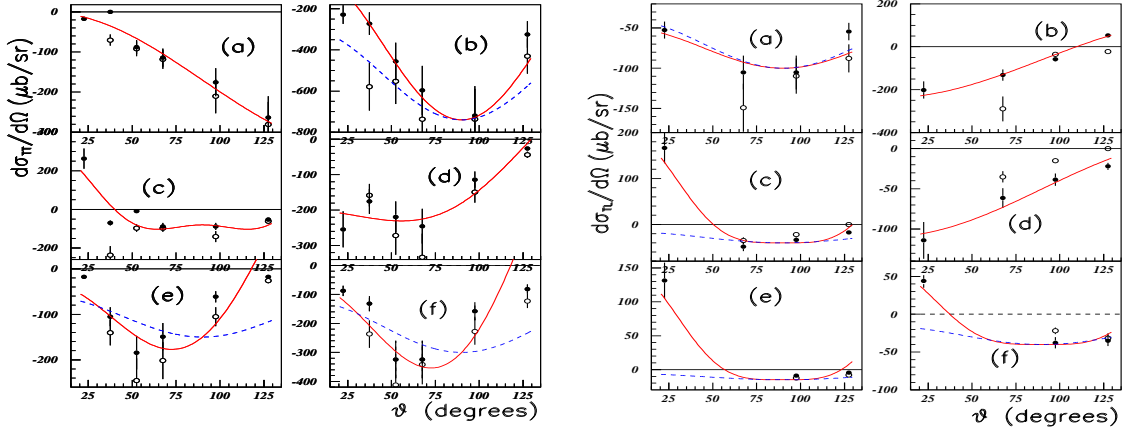


Figure 15: Cross section of the structure functions from the $ep \rightarrow e' n \pi^+$ reaction [11] integrated over the narrow peak surfaces. The six inserts correspond to the following masses: (a) 1136 MeV, (b) 1220 MeV, (c) 1277 MeV, (d) 1339 MeV, (e) 1423 MeV, and (f) 1480 MeV.

narrow resonances. These last may be single-particle or quasi-particle states with more complicated structures than $|q >^3$. They were not observed previously, probably due to the lack of experimental precision. Such suggestion agrees with two observations:

- the mean mass of the several narrow baryons, observed in the $1460 \leq M \leq 1680$ MeV mass range in SPES3 data, are very close to $M=1535$ MeV (S_{11}) and $M=1650$ MeV (S_{11}) for the states which deexcite into $N\pi$ and $N\eta$, and very close to 1520 (D_{13}) and 1600 (ΔP_{33}) for the states which deexcite only into $N\pi$ (see fig. 2),
- the many data observed at JLAB, from the Hall A, or from the CLAS collaboration, are compatible with the presence of several narrow baryonic structures. In some cases, small experimental structures in the mass range between 1.30 GeV and 1.45 GeV, not reproduced by MAID fits, favours our interpretation,
- the structure fits are tentatively presented, since a better experimental resolution is necessary on the one hand, and since such extraction ignores the physical background and interferences on the other hand.

It is therefore difficult to use these angular distributions to suggest quantum numbers and parities of the narrow resonances. Moreover the previous figures show some overlap between structures. If the main part of the overlap is due to physic widths (and not experimental), then possible interferences between them should also be considered.

References

- [1] B. Tatischeff, J. Yonnet, N. Willis *et al.*, Phys. Rev. Lett. **79**, 601 (1997).
- [2] B. Tatischeff, J. Yonnet, M. Boivin *et al.*, Eur. Phys. J. **A 17**, 245 (2003).
- [3] B. Tatischeff, J. Yonnet, M. Boivin *et al.*, Phys. Rev. **C72**, 0304004 (2005)
- [4] H.P. Morsch, M. Boivin, W. Jacobs *et al.*, Phys. Rev. Lett. **69**, 1336 (1992).
- [5] H.P. Morsch, in *Proceedings of the Dixième Journée Thématique de l'IPN d'Orsay (1995)*.
- [6] E.L. Hallin *et al.*, Phys. Rev. **C48**, 1497 (1993).
- [7] V. Olmos de Leon *et al.*, Eur. Phys. J. **A 10**, 207 (2001).
- [8] D. Abbott *et al.*, Phys. Rev. Lett. **82**, 1379 (1999).
- [9] G. Laveissière *et al.* The Hall A Collaboration, arXiv:hep-ex/0406062 (2004).
- [10] G. Laveissière *et al.* The Hall A Collaboration, arXiv:hep-ex/0308009 (2004).
- [11] H. Egiyan *et al.* Phys. Rev. **C73**, 025204 (2006).
- [12] D. Drechsel, S.S. Kamalov, and L. Tiator, Nucl. Phys. **A645**, 145 (1999).